

Sven G. Meuth · Tatjana Kanyshkova  
Peter Landgraf · Hans-Christian Pape · Thomas Budde

## Influence of $\text{Ca}^{2+}$ -binding proteins and the cytoskeleton on $\text{Ca}^{2+}$ -dependent inactivation of high-voltage activated $\text{Ca}^{2+}$ currents in thalamocortical relay neurons

Received: 23 July 2004 / Revised: 3 November 2004 / Accepted: 13 December 2004 / Published online: 13 January 2005  
© Springer-Verlag 2005

**Abstract**  $\text{Ca}^{2+}$ -dependent inactivation (CDI) of high-voltage activated (HVA)  $\text{Ca}^{2+}$  channels was investigated in acutely isolated and identified thalamocortical relay neurons of the dorsal lateral geniculate nucleus (dLGN) by combining electrophysiological and immunological techniques. The influence of  $\text{Ca}^{2+}$ -binding proteins, calmodulin and the cytoskeleton on CDI was monitored using double-pulse protocols (a constant post-pulse applied shortly after the end of conditioning pre-pulses of increasing magnitude). Under control conditions the degree of inactivation ( $34 \pm 9\%$ ) revealed a U-shaped and a sigmoid dependency of the post-pulse current amplitude on pre-pulse voltage and charge influx, respectively. In contrast to a high concentration (5.5 mM) of EGTA ( $31 \pm 3\%$ ), a low concentration (3  $\mu\text{M}$ ) of parvalbumin ( $20 \pm 2\%$ ) and calbindin<sub>D28K</sub> ( $24 \pm 4\%$ ) significantly reduced CDI. Subtype-specific  $\text{Ca}^{2+}$  channel blockers indicated that L-type, but not N-type  $\text{Ca}^{2+}$  channels are governed by CDI and modulated by  $\text{Ca}^{2+}$ -binding proteins. These results point to the possibility that activity-dependent changes in the intracellular  $\text{Ca}^{2+}$ -binding capacity can influence CDI substantially. Furthermore, calmodulin antagonists (phenoxybenzamine,  $22 \pm 2\%$ ; calmodulin binding domain,  $17 \pm 1\%$ ) and cytoskeleton stabilizers (taxol,  $23 \pm 5\%$ ; phalloidin,  $15 \pm 3\%$ ) reduced CDI. Taken to-

gether, these findings indicate the concurrent occurrence of different CDI mechanisms in a specific neuronal cell type, thereby supporting an integrated model of this feedback mechanism and adding further to the elucidation of the role of HVA  $\text{Ca}^{2+}$  channels in thalamic physiology.

**Keywords** Patch clamp ·  $\text{Ca}^{2+}$  channel · Isolated neurons · Thalamus ·  $\text{Ca}^{2+}$ -binding proteins · Cytoskeleton ·  $\text{Ca}^{2+}$ -dependent inactivation

### Introduction

Thalamocortical relay neurons display two typical modes of action potential generation: burst firing with between two and six action potentials riding on a low-threshold  $\text{Ca}^{2+}$  spike during periods of slow-wave sleep and tonic, single-spike activity with trains of action potentials during states of wakefulness [15, 61]. Whilst the role of low-voltage activated (LVA)  $\text{Ca}^{2+}$  channels in rhythmic burst activity is well understood, much less is known about the function of high-voltage activated (HVA)  $\text{Ca}^{2+}$  channels in tonic firing. In general,  $\text{Ca}^{2+}$  in thalamic cells has been regarded traditionally as a common charge carrier. Recent experiments, however, have begun to unravel a complex  $\text{Ca}^{2+}$ -signalling network with interacting extra- and intracellular  $\text{Ca}^{2+}$  sources [11, 50]. Tonic patterns of  $\text{Na}^+/\text{K}^+$  spikes, known to mediate the transfer of sensory information from the periphery to the primary sensory cortex, is supported by activation of HVA  $\text{Ca}^{2+}$  currents,  $\text{Ca}^{2+}$ -induced  $\text{Ca}^{2+}$  release (CICR) from intracellular stores via ryanodine receptors (RyR) and a repolarizing mechanism involving  $\text{Ca}^{2+}$ -dependent  $\text{K}^+$  channels [7, 10, 43]. Furthermore, tonic activity is accompanied by transient increases in the intracellular  $[\text{Ca}^{2+}]$  ( $[\text{Ca}^{2+}]_i$ ) [45, 64] and is coupled to  $\text{Ca}^{2+}$ -dependent inactivation (CDI), thereby limiting the amount of  $\text{Ca}^{2+}$  entering the cell [42, 43]. These data indicate a fine tuning of

S. G. Meuth (✉) · T. Kanyshkova · P. Landgraf · H.-C. Pape  
T. Budde  
Otto-von-Guericke Universität, Medizinische Fakultät,  
Institut für Physiologie, Leipziger Strasse 44,  
39120 Magdeburg, Germany  
E-mail: sven.meuth@gmx.de  
Tel.: +49-391-6715899  
Fax: +49-391-6715819

H.-C. Pape  
Institut für Physiologie I und Institut für Experimentelle Epilepsieforschung, Westfälische Wilhelms-Universität Münster,  
Robert-Koch-Str. 27a, 48149 Münster, Germany

S. G. Meuth  
Neurologische Klinik, Bayerische Julius-Maximilians-Universität,  
Josef-Schneider Str. 11, 97080 Würzburg, Germany

$\text{Ca}^{2+}$ -dependent mechanisms that will help to control intracellular  $\text{Ca}^{2+}$  transients and associated  $\text{Ca}^{2+}$ -signaling processes. Inactivation of  $\text{Ca}^{2+}$  channels is an important component of this complex signalling system. However, the rate and extent of inactivation varies dramatically between  $\text{Ca}^{2+}$  channel subtypes and neuronal cell types [31]. In general,  $\text{Ca}^{2+}$  channels can inactivate by either voltage-dependent (VDI) or  $\text{Ca}^{2+}$ -dependent processes, where CDI represents a classical feedback mechanism between  $\text{Ca}^{2+}$  entry and  $[\text{Ca}^{2+}]_i$  [11, 19, 26, 62].

Experiments in various types of cells have revealed a range of mechanisms mediating CDI. For instance, involvement of the cytoskeleton has been found in cardiac myocytes [34], hippocampal cells [4, 30] and snail neurons [23, 29] and calmodulin has been identified as the  $\text{Ca}^{2+}$  sensor for CDI of L-type and P/Q-type  $\text{Ca}^{2+}$  channels in expression systems [35, 53, 55, 65], whereby these channels are regulated by calmodulin in a lobe-specific manner [39]. To fulfil this function  $\text{Ca}^{2+}$ -free calmodulin and L-type  $\text{Ca}^{2+}$  channels are preassociated as has been shown by fluorescence resonance energy transfer (FRET) two-hybrid mapping [20]. Furthermore, other  $\text{Ca}^{2+}$ -binding proteins like NCS-1 (neuronal  $\text{Ca}^{2+}$  sensor protein 1) or CaBP1 (neuronal  $\text{Ca}^{2+}$ -binding protein 1) modulate HVA  $\text{Ca}^{2+}$  channels in a manner that is markedly different from modulation by calmodulin [37, 57].

In thalamocortical relay neurons CDI is modulated by counterbalancing phosphorylation/dephosphorylation processes involving different kinases [protein kinase A (PKA), calcium-calmodulin (CaM) kinase] and protein phosphatases (PP1, PP2A, calcineurin) [43]. The present study was undertaken to further gain our knowledge of HVA  $\text{Ca}^{2+}$  channel function in the thalamus by probing the influence of  $\text{Ca}^{2+}$ -binding proteins and the cytoskeleton on CDI in thalamocortical relay neurons.

## Materials and methods

### Preparation

**Long Evans rats (12-to 20-day-old)** were decapitated under halothane anaesthesia, the brains removed quickly and placed in cold, oxygenated artificial cerebrospinal fluid (ACSF) containing (mM): sucrose, 210; 1,4-piperazinediethanesulphonic acid (PIPES), 20; KCl, 2.4;  $\text{MgCl}_2$ , 10;  $\text{CaCl}_2$ , 0.5; dextrose, 10; pH 7.25 with NaOH. Thalamic slices (400–500  $\mu\text{m}$ ) were obtained from coronal sections according to procedures similar to those reported previously [9, 42, 43]. In brief, slices were cut on a vibratome (Model 1000, Ted Pella, Redding, Calif., USA), transferred to a spinner flask and incubated for 25–30 min at 30 °C in an oxygenated solution containing trypsin (0.5–1 mg/ml, Sigma, Taufkirchen, Germany) and (mM): NaCl, 120; KCl, 5;  $\text{MgCl}_2$ , 3;  $\text{CaCl}_2$ , 1; PIPES, 20; dextrose, 25; pH adjusted to 7.35 with NaOH.

### Electrophysiology

Single neurons were obtained by trituration and placed under an inverted microscope (Axiovert 135, Zeiss, Jena, Germany) as described previously [42, 43]. **Whole-cell recordings** were performed at **room temperature (21–23 °C)** using borosilicate glass pipettes (GC150TF-10, Clark Electromedical Instruments, Pangbourne, UK) connected to an EPC-7 amplifier (E.S.F. electronics, Friedland, Germany). The typical electrode resistance was 2–5  $\text{M}\Omega$ , while **access resistance was 3–8  $\text{M}\Omega$** . Series resistance compensation was routinely used ( $\geq 40\%$ ). With a **holding potential of –50 mV**, voltage-clamp experiments were governed by pClamp software, operating via an interface (Digidata 1200, Axon Instruments, Foster City, Calif., USA). For all recordings the following solutions were used. (1) Extracellular solution (mM): NaCl, 112; CsCl, 4; KCl, 1; HEPES, 10; dextrose, 10;  $\text{MgCl}_2$ , 1;  $\text{CaCl}_2$ , 5.0; tetrodotoxin (TTX), 0.001; tetraethylammonium (TEA-Cl), 20; 4-aminopyridine (4-AP), 6; pH 7.35 with NaOH. (2) Intracellular solution: Cs-gluconate, 85;  $\text{Cs}_3$ -citrate, 10; NaCl, 10; KCl, 1; EGTA, 1.1;  $\text{CaCl}_2$ , 0.1;  $\text{MgCl}_2$ , 0.25; HEPES, 10; TEA-Cl, 15; Mg-ATP, 3; Na<sub>2</sub>-GTP, 0.5; pH 7.25 with CsOH. In one set of experiments EGTA and  $\text{CaCl}_2$  were set to 5.5 and 0.5 mM, respectively. In some experiments EGTA and  $\text{CaCl}_2$  were removed from the pipette solution.

In a subset of experiments, peptides and purified proteins were added to the internal solution using the back-filling technique. According to [54] the calculated rates of diffusional exchange between small cells and a measuring patch pipette were: calmodulin binding domain (2.3 kDa) 2.4 min; lysozyme (12 kDa) 4.0 min; parvalbumin (13 kDa) 4.2 min; calbindin (28 kDa) 5.4 min; calretinin (30 kDa) 5.6 min (assuming an average access resistance of 5  $\text{M}\Omega$  and an average cell capacitance of 14 pF). Purified  $\text{Ca}^{2+}$ -binding proteins and lysozyme were obtained from Swant and Sigma, respectively.

The time course of inactivation of  $\text{Ca}^{2+}$  inward currents was described by approximating the current wave form to the function:

$$I = A_0 + A_1 \cdot e^{-\frac{t}{\tau_1}} + A_2 \cdot e^{-\frac{t}{\tau_2}} + \dots$$

where amplitude coefficients and time constants of current decay are  $A_0$ – $A_n$  and  $\tau_1$ – $\tau_n$ , respectively. The inactivation ratio ( $R_{\text{inact}}$ ) was calculated using the equation:

$$R_{\text{inact}} = \frac{B_1}{B_0}$$

where  $B_1$  represents the current amplitude at the end of the pulse and  $B_0$  the peak current amplitude (Fig. 1B, inset) [32]. The degree of inactivation ( $D_{\text{inact}}$ ; in percent; see Fig. 1C, lower panel) during double-pulse protocols was determined by using the following equation:

$$D_{\text{inact}} = \left(1 - \frac{C_1}{C_0}\right) \cdot 100$$

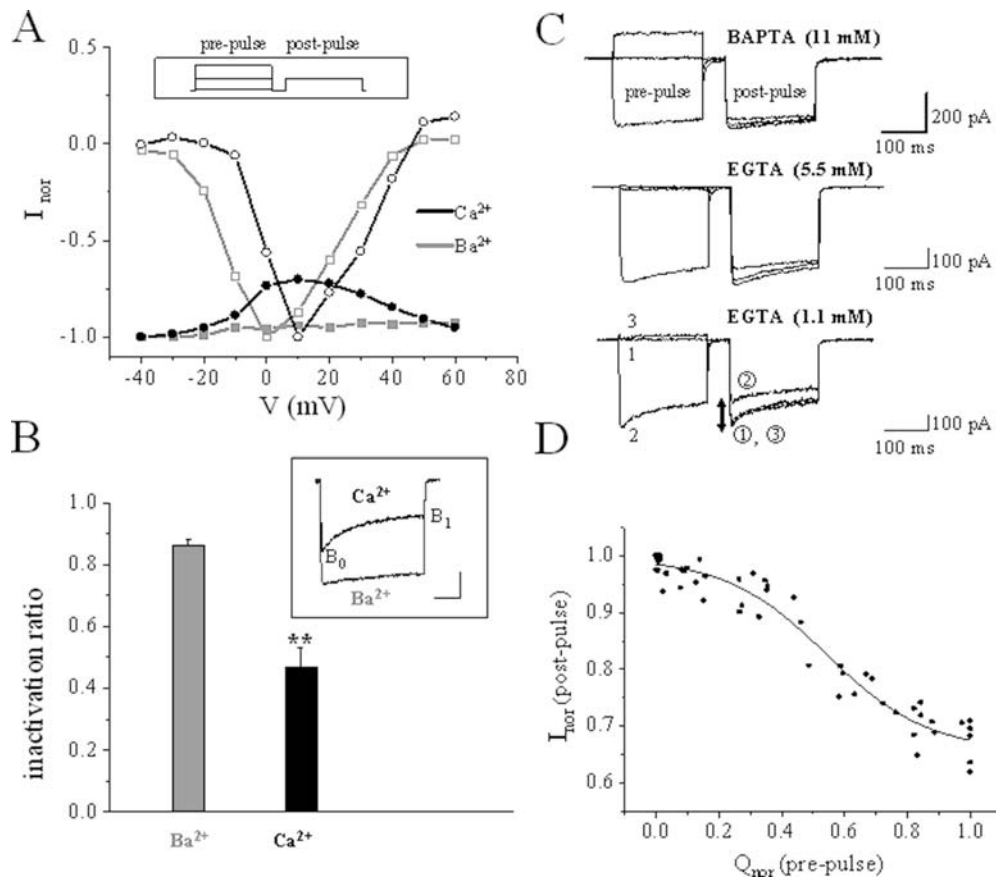


**Fig. 1A–D**  $\text{Ca}^{2+}$ -dependent inactivation (CDI) of high-voltage activated (HVA)  $\text{Ca}^{2+}$  current in thalamic relay neurons. **A** Normalized current/voltage ( $I/V$ ) relationship of the pre-pulse (open symbols) and the dependency of the post-pulse peak amplitude on the pre-pulse potential (closed symbols) under different recording conditions for two individual cells. Currents were evoked by double-pulse protocols (pre-pulse was varied between  $-40$  and  $+60$  mV, post-pulse  $+10$  mV) under control conditions ( $\text{Ca}^{2+}$ , circles, black lines) and with  $\text{Ba}^{2+}$  as main charge carrier ( $\text{Ba}^{2+}$ , squares, grey lines). **B** Average inactivation ratio ( $B_1/B_0$ , see text) of HVA currents with  $\text{Ca}^{2+}$  and  $\text{Ba}^{2+}$ . *Inset*: current traces recorded with charge carriers  $\text{Ca}^{2+}$  and  $\text{Ba}^{2+}$  demonstrating different inactivation of HVA  $\text{Ca}^{2+}$  currents evoked

by stepping from  $-50$  to  $+10$  mV. Scale bars: 50 ms and 200 pA.  $**P < 0.01$ . **C** Double-pulse protocols (see inset in **A**) consisting of a conditioning pre-pulse (200 ms) to varying membrane potentials, a brief gap (50 ms,  $-50$  mV) and a test pulse (200 ms) to a fixed membrane potential ( $+10$  mV) recorded with 11 mM BAPTA (upper panel), 5.5 mM EGTA (middle panel) or 1.1 mM EGTA (lower panel) included to the pipette solution. Current traces conditioned by pre-pulses to  $-40$ ,  $+10$ , and  $+50$  mV are shown. Corresponding pre- and post-pulses under control conditions are indicated by numbers. The double-headed arrow shows the degree of inactivation. **D** Normalized post-pulse peak current amplitude/pre-pulse charge ( $I/Q$ ) relationship of five representative cells

where  $C_1$  is the peak of the post-pulse current when the pre-pulse elicited a maximal inward current (i.e.  $+10$  mV and  $0$  mV with  $\text{Ca}^{2+}$  and  $\text{Ba}^{2+}$  as charge carriers, respectively) and  $C_0$  the peak of the post-pulse current when the pre-pulse elicited no current (i.e.  $-40$  mV).

The current/charge ( $I/Q$ ) relationship was determined by integrating  $\text{Ca}^{2+}$  inwards currents elicited by pre-pulses with respect to time and plotting the calculated charge as functions of the peak amplitude of the corresponding post-pulse. Results are presented as **mean  $\pm$  SEM**. Substance effects were tested for significance using a modified  $t$ -test for small samples [16]. Differences were considered significant if  $P < 0.05$ .

#### Immunocytochemistry

Slices were stained according to [16]. Acutely isolated dorsal lateral geniculate nucleus (dLGN) cells adhered

to poly-L-lysine-coated glass slides or freely floating thalamic slices (60  $\mu\text{m}$  thick) were incubated in PBS (pH 7.4) containing 0.4% glutaraldehyde for 10 min. Preincubation with the appropriate normal serum (1 h, 10% in PBS) was followed by the primary antiserum (18 h at room temperature) against calmodulin (Calbiochem, 1:200), calbindin (Sigma, 1:1,000 for histochemistry, 1:2,000 for protein blots) calretinin (Swant, 1:3,000 for histochemistry, 1:2,000 for protein blots), or parvalbumin (Swant, 1:1,000 for histochemistry, 1:750 for protein blots). The primary antibodies were tagged by appropriate biotinylated secondary antisera (Vector Labs, Burlingame, Calif., USA; BA-5000, 1.5 h, 1:200) followed by incubation with avidin-biotin-complexed horseradish peroxidase (Vector Labs, PK 4000, 1:100, 1.5 h). Between steps, slides were rinsed 3 times in PBS. Antibodies were diluted in PBS containing 2% normal serum, 0.3% Triton, 2% BSA. Peroxidase activity was

initiated by adding PBS containing 0.05% 3,3'-diaminobenzidine, 0.01%  $\text{H}_2\text{O}_2$ , 0.02%  $(\text{NH}_4)_2\text{Ni}(\text{SO}_4)_2$  and 0.025%  $\text{CoCl}_2$  resulting in an enhanced dark grey-to-black staining of positively labelled neurons. For slices the intensifying step was not performed. After stopping the reaction isolated cells and tissue were dehydrated and cover-slipped in DePeX (Serva, Heidelberg, Germany) mounting medium.

As a negative control, antibodies were preincubated with the control antigen peptide supplied by the manufacturer. Under these conditions no positive immunological signal was detected. In addition, occlusion of the primary antibody from the staining procedure revealed no positive immunological signal. For each subtype antibody reactions were repeated 4 times. One set of sections was Nissl-stained and used to evaluate the overall density of cells in dLGN tissue.

### Western blotting procedures

Thalamic and skeletal muscle tissue extracted from Long Evans rats at postnatal days (P)5, P10, P12, P13, P14, P20 and P30 was homogenized in a buffer containing 1% 3-[(3-chloramidopropyl)-dimethylammonio]-propanesulphonate (CHAPS, Merck, Darmstadt, Germany) and a cocktail of protein inhibitors [calpain-I inhibitor, calpain-II inhibitor, leupeptin, phenylmethylsulphonyl fluoride (PMSF) and aprotinin; Boehringer, Mannheim, Germany]. Via centrifugation (10 min at 3,000 g) proteins were separated and determined according to Bradford [8]. Protein samples of 50 or 100  $\mu\text{g}$  were lyophilized, dissolved in SDS-sample buffer and 50 mM dithiothreitol added (calbindin, calretinin). For electrophoretic studies of parvalbumin, calbindin and calretinin a 4–16% gradient tricine gel was used. After electrophoresis proteins were transferred for 14–16 h at 100 mA to nitrocellulose (0.45  $\mu\text{m}$ , Schleicher and Schuell; Dassel, Germany). Thereafter the transfer was blocked with 0.2% Tween 20 and 1% BSA in TRIS-buffered saline for 1 h.

## Results

### CDI of HVA currents

HVA  $\text{Ca}^{2+}$  currents were evoked in dLGN relay neurons by stepping the membrane potential for 200 ms from  $-50$  to  $+10$  mV (Fig. 1B inset, black current trace). The total HVA  $\text{Ca}^{2+}$  current activated rapidly and then declined rapidly revealing an inactivation ratio of  $0.47 \pm 0.06$  ( $n = 22$ ; Fig. 1B). Time constants of inactivation were derived from 1.2-s pulses and were characterized by a biexponential time course with  $\tau_1 = 56 \pm 6$  and  $\tau_2 = 726 \pm 88$  ms ( $n = 7$ ; data not shown) [42]. In double-pulse experiments (see inset in Fig. 1A) performed under control conditions (Fig. 1C, 1.1 mM EGTA) conditioning pre-pulses of increasing amplitude

( $-40$  to  $+60$  mV, 10-mV increments) revealed the typical current/voltage ( $I/V$ ) relationship for HVA  $\text{Ca}^{2+}$  currents in relay neurons (Fig. 1A, open circles). Moreover, the peak amplitude of the analysing post-pulse revealed an (inverted) U-shaped dependency on the pre-pulse potential (Fig. 1A, closed circles), indicating CDI [42, 43]. The degree of inactivation (indicated by the double-headed arrow in Fig. 1C) averaged  $34 \pm 9\%$  ( $n = 9$ ; Fig. 2E). To obtain a more direct measure of the influence of  $\text{Ca}^{2+}$  influx during the pre-pulse on CDI, the  $I/Q$  curve was constructed and revealed a sigmoidal dependency of the post-pulse amplitude on  $\text{Ca}^{2+}$  influx (Fig. 1D). With  $\text{Ba}^{2+}$  as main charge carrier the HVA current activated rapidly and then inactivated slowly (Fig. 1A inset). Long current traces (1.2 s) indicated a monoexponential decay with  $\tau_1 = 832 \pm 46$  ms (data not shown) [42]. The inactivation ratio was  $0.86 \pm 0.02$  ( $n = 18$ ; Fig. 1B). Double-pulse protocols revealed a hyperpolarizing shift in the  $I/V$  relationship of HVA current (Fig. 1A) and a reduction in the degree of inactivation to  $12 \pm 4\%$  ( $n = 6$ , Fig. 1A).

Since standard whole-cell patch-clamping is accompanied by altered  $\text{Ca}^{2+}$  binding conditions in the recorded neurons, we next tried to assess the basal degree of CDI and the effect of exogenous  $\text{Ca}^{2+}$  buffers. For double-pulse protocols applied within the first 90 s after establishing the whole-cell configuration, incomplete equilibration between the pipette and the cytosol was assumed [25], thereby giving a rough estimate of the basal level of CDI. The mean degree of inactivation under these conditions ( $39 \pm 6\%$ ,  $n = 4$ ; data not shown) was not significantly different from recordings obtained 5–10 min after rupture of the cell membrane with zero ( $38 \pm 2\%$ ,  $n = 3$ ; data not shown), 1.1 mM ( $34 \pm 4\%$ ,  $n = 8$ ; Fig. 1C) or 5.5 mM ( $31 \pm 3$ ,  $n = 6$ ; Fig. 1C) EGTA added to the internal solution. For comparison, 11 mM BAPTA as intracellular  $\text{Ca}^{2+}$  buffer significantly reduced the degree of inactivation to  $15 \pm 1\%$  ( $n = 8$ ; Fig. 1C). These data indicate that rather large changes in the bulk intracellular  $\text{Ca}^{2+}$  binding capacity and kinetic are necessary to influence CDI under our experimental conditions.

### Influence of calmodulin on CDI

Since calmodulin has been suggested as the sensor for CDI [35, 53, 55, 65], the expression of calmodulin was monitored in dLGN cells using an anti-calmodulin antibody. A total of 238 cells comprising local interneurons and relay neurons were inspected. All cells were identified through morphological criteria [49] and were immunopositive for calmodulin (Fig. 2D).

To determine whether calmodulin is involved in CDI in relay neurons, two well-known calmodulin inhibitors were tested [14, 59]. Addition of the irreversible calmodulin antagonist phenoxybenzamine (20  $\mu\text{M}$ ) to the bathing solution significantly increased the peak amplitude of HVA  $\text{Ca}^{2+}$  current by  $53 \pm 12\%$  ( $n = 10$ ; Fig. 2E



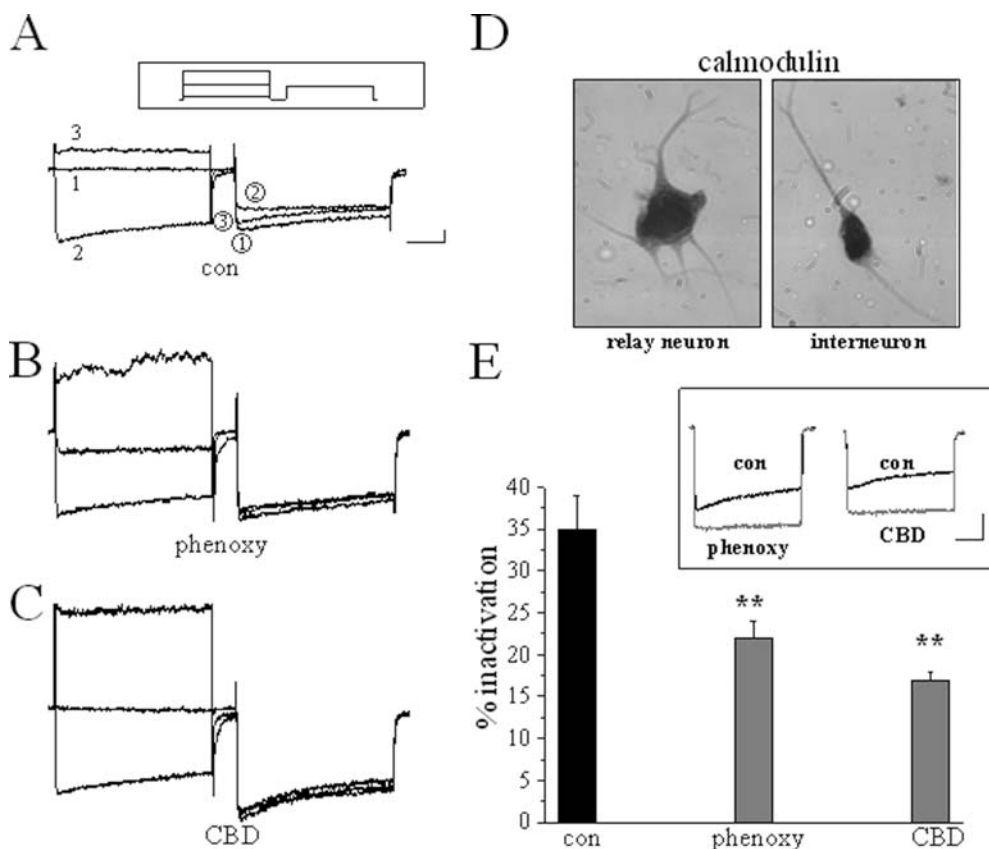


**Fig. 2A–E** Contribution of calmodulin to CDI of  $\text{Ca}^{2+}$  currents. **A–C** Current traces evoked by double-pulse protocols under control conditions (**A**), during bath application of phenoxybenzamine (20  $\mu\text{M}$ , **phenoxy**; **B**) and 10 min after establishing the whole-cell configuration using a pipette backfilled with a solution containing the calmodulin binding domain (200  $\mu\text{M}$ , **CBD**; **C**). Current traces conditioned by pre-pulses to  $-40$ ,  $+10$  and  $+50$  mV are shown. Corresponding pre- and post-pulses under control conditions are indicated by numbers. Scale bars for **A–C**: 100 pA and 50 ms.

**D** Acutely isolated dorsal lateral geniculate nucleus (dLGN) cells stained for the presence of calmodulin. Representative examples of a relay neuron (*left*) and an interneuron (*right*). **E** Mean ( $\pm$  SEM) degree of inactivation under control conditions and in the presence of phenoxybenzamine and CBD; \*\* $P < 0.01$ . *Inset*: HVA currents evoked by depolarizing voltage steps under control conditions (*black traces*) and during application of phenoxybenzamine (20  $\mu\text{M}$ ; *left panel, grey trace*) and calmodulin binding domain (200  $\mu\text{M}$ , *right panel, grey trace*). Scale bars: 200 pA and 50 ms

inset). The degree of inactivation seen in double-pulse protocols (Fig. 2B) was significantly reduced to  $22 \pm 2\%$  ( $n = 5$ ; Fig. 2E) and the inactivation ratio was  $0.81 \pm 0.02$  ( $n = 5$ ). A similar effect was evoked by intracellular application of the calmodulin binding domain of CaMK II (200  $\mu\text{M}$ ), a potent calmodulin inhibitor [52]. The peak amplitude of HVA  $\text{Ca}^{2+}$  currents significantly increased about 4 min after establishing of the whole-cell recording by  $32 \pm 2\%$  ( $n = 7$ ; Fig. 2E inset). Double-pulse protocols under these conditions (Fig. 2C) revealed a significantly reduced degree of inactivation ( $17 \pm 1\%$ ,  $n = 7$ ; Fig. 2E), corresponding to an inactivation ratio of  $0.86 \pm 0.04$  ( $n = 3$ ). Taken together, these results indicate the involvement of calmodulin in CDI in relay neurons.

$\text{Ca}^{2+}$ -binding proteins: expression in the dLGN and influence on CDI

Next, the expression and effects of endogenous  $\text{Ca}^{2+}$ -binding proteins were analysed. Immunohistochemical

studies determining the expression of calbindin- $\text{D}_{28\text{K}}$  (CB), calretinin (CR) and parvalbumin (PV) were performed on dLGN slices (60  $\mu\text{m}$  thick sections from 14- to 21-day-old rats). Alternate sections were Nissl-stained and revealed an overall density of neurons in the dLGN of  $5,434 \pm 326$  cells/ $\text{mm}^2$  (measured in six slices from three animals).

Western blot analysis of dLGN tissue using a CB-specific antibody revealed a band of 28 kDa present throughout postnatal development (Fig. 3A). In dLGN slices, CB-immunoreactive cells were found at a density of  $183 \pm 41$  cells/ $\text{mm}^2$  ( $n = 3$ ), indicating that about 3% of neurons in dLGN express CB. Among the CB-positive structures small (soma diameter 8–12  $\mu\text{m}$ ) bipolar cells (Fig. 3A) and, to a much lesser extent, large (soma diameter 15–25  $\mu\text{m}$ ) multipolar cells could be identified, most likely representing interneurons and relay neurons, respectively [21, 24, 48].

In Western blots CR was represented by a band of 30 kDa and was present from P5 to P30 in the dLGN (Fig. 3A). After immunohistochemistry, CR-labelled neurons were found at a density of  $488 \pm 32$  cells/ $\text{mm}^2$

( $n=3$  slices), indicating that about 9% of dLGN neurons express CR. Size and shape of CR-positive cells were indicative of interneurons (Fig. 3A).

PV expression was monitored in the dLGN in comparison to skeletal muscle tissue, which is known to express high concentrations of PV [5]. In dLGN, PV displayed a molecular mass of 13 kDa, identical to that in muscle (Fig. 3A). In comparison to PV in skeletal muscle tissue, levels of PV in dLGN were low but detectable throughout postnatal development. Following immunohistochemistry, fibres and neurons were positively stained for PV. Size and shape of PV-positive cells were typical of relay neurons (Fig. 3A). Analysis of PV expression in dLGN slices and thalamic cell cultures (data not shown) indicated that  $79 \pm 1\%$  (a total of 1687 cells were counted on seven different slides) of thalamic cells and 100% of cultured relay neurons (a total of 49 relay neurons were identified in 12 different cultures) were PV positive, respectively. Taken together, these findings indicate that all three  $\text{Ca}^{2+}$ -binding proteins are expressed in dLGN tissue at the ages used for electrophysiological recordings.

To determine whether  $\text{Ca}^{2+}$ -binding proteins expressed in dLGN modulate CDI, purified CB, CR and PV (1  $\mu\text{M}$  each) were co-infused into relay neurons using the back-filling technique. The HVA  $\text{Ca}^{2+}$  current increased significantly (by  $90 \pm 6\%$ ,  $n=4$ ) within 5–10 min after establishing the whole-cell configuration (Fig. 3C inset, left panel). The final inactivation ratio was  $0.76 \pm 0.06$  ( $n=3$ ; data not shown). When double-pulse protocols were delivered under these conditions, there was a significant reduction in the degree of inactivation to  $21 \pm 1\%$  ( $n=4$ ; data not shown).

The effect of each  $\text{Ca}^{2+}$ -binding protein was then investigated separately. In general, the effect of  $\text{Ca}^{2+}$ -binding proteins may result from an increase in intracellular  $\text{Ca}^{2+}$ -binding capacity or  $\text{Ca}^{2+}$  signalling to intracellular target molecules. PV is believed to serve solely as a  $\text{Ca}^{2+}$  buffer [18]. First, purified PV (3  $\mu\text{M}$ ) was added to the pipette solution and applied using the back-filling technique. The effect on HVA  $\text{Ca}^{2+}$  current amplitude and the degree of inactivation exerted by double-pulse protocols were similar to the combined effect of all three  $\text{Ca}^{2+}$ -binding proteins, with a  $92 \pm 5\%$  ( $n=4$ ; Fig. 3C inset) increase in current amplitude and a significant reduction in the degree of inactivation to  $20 \pm 2\%$  ( $n=4$ ; Fig. 3C). In addition the inactivation ratio as a measure of time-dependent inactivation was increased to  $0.81 \pm 0.01$  ( $n=3$ ). For comparison, either CR (3  $\mu\text{M}$ ) or CB (3  $\mu\text{M}$ ) were added to the pipette solution in separate sets of experiments and the degree of inactivation was significantly decreased for CB ( $24 \pm 4\%$ ,  $n=4$ ; Fig. 3C) but not CR ( $30 \pm 2\%$ ,  $n=3$ ; Fig. 3C). Taken together, these data indicate that rather small increases in the amount of  $\text{Ca}^{2+}$ -binding proteins can reduce CDI significantly in dLGN relay neurons.

To demonstrate that the effects described above are a consequence of  $\text{Ca}^{2+}$  binding rather than introduction of a protein per se, lysozyme (3  $\mu\text{M}$ ) was added to the

pipette solution. Lysozyme (12 kDa) is similar in size to PV (13 kDa) but does not bind  $\text{Ca}^{2+}$  effectively [12]. Following introduction of lysozyme into relay neurons, peak HVA  $\text{Ca}^{2+}$  current amplitude was stable with time and the degree of CDI ( $33 \pm 1\%$ ,  $n=4$ ; Fig. 3C) was not significantly different from control cells.

Relay neurons express a set of at least four different HVA  $\text{Ca}^{2+}$  current components, namely L-, N-, P/Q- and R-type, of which only L- and Q-type currents are governed by CDI [42, 43]. We therefore tried to assess the contribution L- and N-type currents, as prototypical CDI-sensitive and CDI-insensitive components, respectively, to the effects of  $\text{Ca}^{2+}$ -binding proteins. Under control conditions the degree of inactivation was reduced significantly to  $19 \pm 1\%$  ( $n=8$ ; Fig. 3B,D) during application of nifedipine (1  $\mu\text{M}$ ), an L-type-specific blocker, but unchanged ( $32 \pm 1\%$ ,  $n=7$ ; Fig. 3B,D) by application of  $\omega$ -conotoxin GVIA (1  $\mu\text{M}$ ), an N-type-specific blocker. PV (3  $\mu\text{M}$ ) was then applied to relay neurons via the recording pipette in the presence of subtype-specific blockers. Under these conditions the degree of inactivation was significantly reduced in the presence of  $\omega$ -conotoxin GVIA ( $21 \pm 4\%$ ,  $n=3$ ; Fig. 3B,D) but remained unchanged in the presence of nifedipine ( $18 \pm 4\%$ ,  $n=4$ ; Fig. 3B,D). From these data it can be concluded that CDI of L-type  $\text{Ca}^{2+}$  channels is inhibited by rather small increases in intracellular PV concentration.

#### Action of agents interfering with the cytoskeleton

To test the role of the cytoskeleton in CDI, agents that act on microfilament (phalloidin and cytochalasin) and microtubule (taxol and colchicine) components of the cytoskeleton were applied. When the cytoskeletal stabilizers taxol (2  $\mu\text{M}$ ) and phalloidin (100  $\mu\text{M}$ ) were both added to the pipette solution, the degree of CDI was significantly reduced to  $13 \pm 3\%$  ( $n=4$ ; Fig. 4B,E), corresponding to an inactivation ratio of  $0.8 \pm 0.01$  ( $n=4$ ). When applied separately, phalloidin and taxol reduced CDI to  $23 \pm 5\%$  ( $n=4$ ; Fig. 4C,E) and  $15 \pm 3\%$  ( $n=4$ ; Fig. 4D,E), corresponding to inactivation ratios of  $0.79 \pm 0.04$  ( $n=4$ ) and  $0.88 \pm 0.01$  ( $n=4$ ), respectively. In contrast, the cytoskeletal disrupters colchicine (100  $\mu\text{M}$ ) and cytochalasin B (50  $\mu\text{M}$ ) had no significant effect on the degree of CDI ( $n=4$ ; Fig. 4A,E), as confirmed by an inactivation ratio of  $0.54 \pm 0.02$  ( $n=4$ ). No changes in holding current or membrane resistance were observed during application of cytoskeletal agents. These data indicated that agents interfering with the normal ability of the cytoskeleton for self-sustained reconstruction reduce CDI.

#### Discussion

The inactivation of HVA  $\text{Ca}^{2+}$  currents in thalamic relay neurons displays several characteristics of a

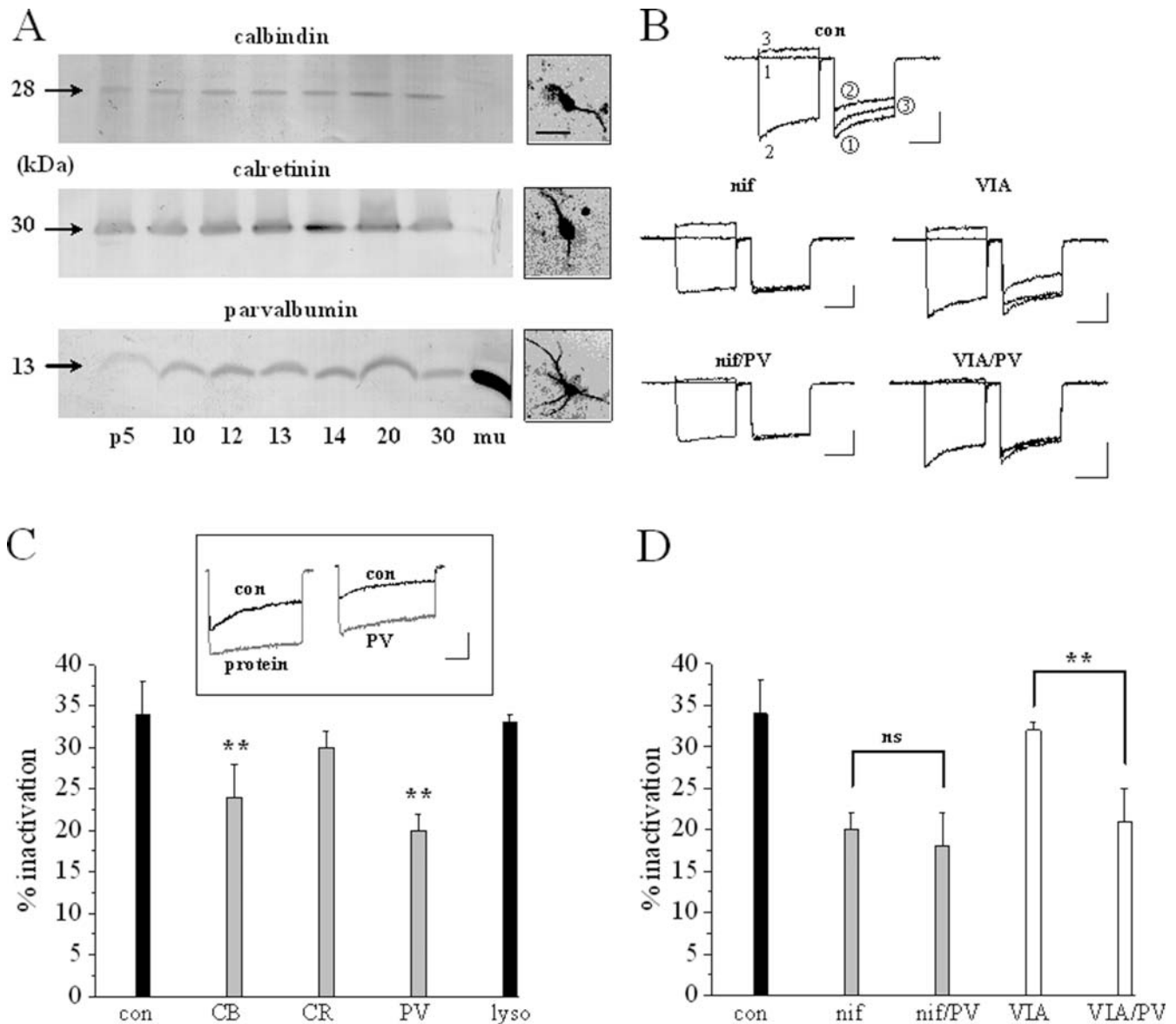


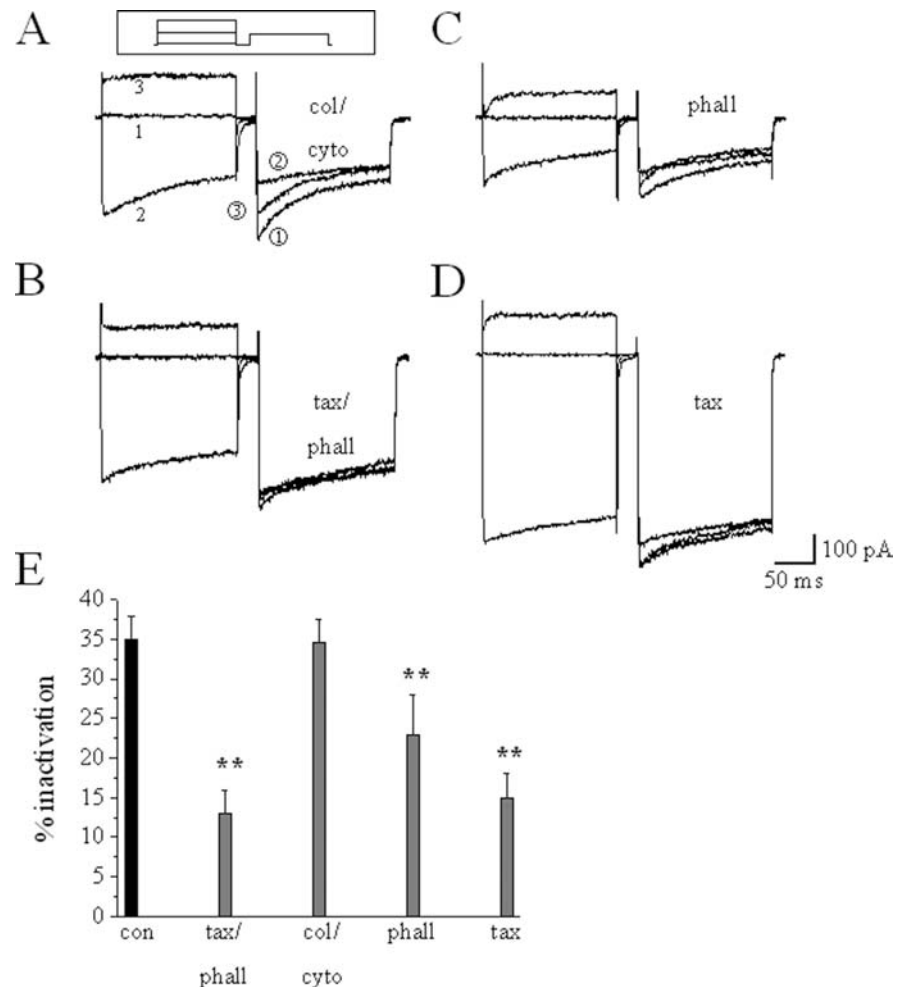
**Fig. 3A–D** Calbindin, calretinin and parvalbumin expression and influence on CDI of HVA  $\text{Ca}^{2+}$  currents. **A** Western blot analysis of calbindin (upper panel), calretinin (middle panel) and parvalbumin (lower panel) expression in dLGN at postnatal days 5–30. Muscle tissue (*mu*) was used for comparison. Arrows indicate the molecular weight of the immunoreactive protein band. Insets show enlarged immunoreactive neurons from rat dLGN slices stained for the presence of calbindin (upper inset), calretinin (middle inset) and parvalbumin (lower inset). Scale bar: 25  $\mu\text{m}$  (calbindin, calretinin) and 40  $\mu\text{m}$  (parvalbumin). **B** HVA  $\text{Ca}^{2+}$  current traces evoked by double-pulse protocols recorded under control conditions (*con*, upper panel), during extracellular application of nifedipine (*nif*, middle left panel) and  $\omega$ -conotoxin GVIA (*VIA*, middle right panel) and extracellular application of  $\text{Ca}^{2+}$  channel blockers in combination with intracellular perfusion with parvalbumin (*PV*, lower left panel: nifedipine and parvalbumin; lower right panel:  $\omega$ -conotoxin GVIA and parvalbumin). Current traces conditioned by pre-pulses to  $-40$ ,  $+10$

and  $+50$  mV are shown. Corresponding pre- and post-pulses under control conditions are indicated by numbers. Scale bars: 200 pA/100 ms under control conditions and 100 pA/100 ms for all other panels. **C** Mean ( $\pm$ SEM) degree of inactivation as determined by means of double-pulse protocols 10 min after infusion of the cells using a pipette back-filled with calbindin (*CB*), calretinin (*CR*), parvalbumin (*PV*) or lysozyme (*lyso*) and under control conditions (*con*).  $**P < 0.01$ . Inset: superimposed current traces recorded 1 (*con*) and 10 min after establishing the whole-cell configuration with a mixture of the three  $\text{Ca}^{2+}$ -binding proteins (1  $\mu\text{M}$  each, *protein*) or parvalbumin (3  $\mu\text{M}$ , *PV*) alone. Scale bars: 50 ms and 200 pA. **D** Mean ( $\pm$ SEM) degree of inactivation as determined by means of double-pulse protocols under control conditions, application of nifedipine, nifedipine in combination with intracellular perfusion with parvalbumin, application of  $\omega$ -conotoxin GVIA and application of  $\omega$ -conotoxin GVIA in combination with intracellular perfusion of parvalbumin.  $**P < 0.01$

$\text{Ca}^{2+}$ -mediated process. First, in double-pulse experiments, the peak of post-pulse currents revealed an (inverted) U-shaped dependence on the pre-pulse

potential and a sigmoidal dependency on the charge influx during the pre-pulse. Second, all inactivation parameters tested (i.e. inactivation time constants, the

**Fig. 4A–E** Involvement of the cytoskeleton in CDI of HVA  $\text{Ca}^{2+}$  currents. **A–D** HVA  $\text{Ca}^{2+}$  current traces evoked by double-pulse protocols recorded 10 min after infusion of the cells with colchicine/cytochalasin (*col/cyto*; **A**), taxol/phalloidin (*tax/phall*; **B**), phalloidin (*phall*; **C**) and taxol (*tax*; **D**). Current traces conditioned by pre-pulses to  $-40$ ,  $+10$  and  $+50$  mV are shown. Corresponding pre- and post-pulses during application of colchicine/cytochalasin are indicated by numbers. **E** Mean ( $\pm$ SEM) degree of inactivation obtained by double-pulse protocols (abbreviations as above;  $**P < 0.01$ )



degree of inactivation measured in double-pulse protocols and the inactivation ratio) were influenced significantly by the charge carrier used, with  $\text{Ca}^{2+}$  being more effective than  $\text{Ba}^{2+}$ . Third, introduction of  $\text{Ca}^{2+}$  buffers reduced CDI significantly.

#### The role of $\text{Ca}^{2+}$ -binding proteins

It has been shown previously that the introduction of exogenous synthetic  $\text{Ca}^{2+}$  chelators into relay neurons reduces CDI [42]. Here we extend this finding by demonstrating that purified  $\text{Ca}^{2+}$ -binding proteins affect CDI differently in these cells. While PV and CB reduced CDI significantly, CR had no effect. It is interesting to note that PV, the expression of which was demonstrated in relay neurons, exerts the strongest effect on CDI. The action of PV is most likely based on  $\text{Ca}^{2+}$  buffering, as PV is generally seen as a pure  $\text{Ca}^{2+}$  buffer [18]. Since CB and CR are believed to also function as  $\text{Ca}^{2+}$  signalling proteins [22, 27, 40], the mode of action of CB may be different. In any case, the effectiveness of low concentrations (3  $\mu\text{M}$ ) of PV and CB indicates that these proteins reach sufficiently high levels around the point of

$\text{Ca}^{2+}$  entry to buffer entering  $\text{Ca}^{2+}$  effectively and is even consistent with a close physical association between PV and/or CB and  $\text{Ca}^{2+}$  channels. In this respect it is interesting to note that other EF-hand  $\text{Ca}^{2+}$ -binding proteins (calmodulin, sorcin) have been shown to associate tightly with  $\text{Ca}^{2+}$  and  $\text{K}^{+}$  channels [20, 38, 44]. Furthermore, the finding that rather small amounts of  $\text{Ca}^{2+}$ -binding proteins are sufficient to disrupt CDI effectively has been described before in hippocampal granule cells, where a low concentration (20  $\mu\text{M}$ ) of exogenous CB substantially reduces this type of feedback coupling [46].

Due to their ability to buffer intracellular free  $\text{Ca}^{2+}$  effectively during neuronal excitation [17],  $\text{Ca}^{2+}$ -binding proteins are also expected to be neuroprotective [63]. The finding of an activity-dependent expression of PV [51] and CB [3] indicates a positive feedback between these two functions. It should be pointed out, however, that down-regulation of  $\text{Ca}^{2+}$ -binding proteins can also act in a neuroprotective manner, as indicated in surviving granule cells of the sclerotic human hippocampus where the loss of CB reduces the amount of  $\text{Ca}^{2+}$  influx since the process of CDI is fully active under these conditions [46]. These findings



indicate a complex correlation between the content of calcium-binding proteins and activity-dependent neuronal vulnerability.

The introduction of exogenous  $\text{Ca}^{2+}$  buffers via the recording pipette raises the question as to the degree of CDI under basal physiological conditions. The finding that the percentage of CDI shortly after rupture of the cell membrane, under EGTA-free conditions and in the presence of 1.1 mM as well as 5.5 mM EGTA was not significantly different may indicate that about 35 % inactivation may approximate the physiological condition. Even large increases in the concentration of EGTA, which does not interfere with  $\text{Ca}^{2+}$  diffusion in channel-associated  $\text{Ca}^{2+}$  microdomains [47] were not able to diminish CDI. This conclusion is corroborated by the finding that high concentrations of BAPTA, which does interfere with  $\text{Ca}^{2+}$  microdomains [47], effectively inhibit CDI. The action of low concentrations of  $\text{Ca}^{2+}$ -binding proteins is thus very different from that of high EGTA loads, thereby supporting the conclusion of a close association of  $\text{Ca}^{2+}$ -binding proteins to the  $\text{Ca}^{2+}$  channel complex and raising the possibility that small changes in protein expression levels effectively alter CDI. On the other hand, the occurrence of prominent CDI in cells expressing PV may indicate that endogenous  $\text{Ca}^{2+}$ -binding proteins play a minor role in CDI. Future studies utilizing PV and CB knock-out mice, determining the  $\text{Ca}^{2+}$  binding ratio of relay neurons, quantifying basal  $\text{Ca}^{2+}$  binding protein expression levels and determining the spatial distance between  $\text{Ca}^{2+}$  channels and  $\text{Ca}^{2+}$ -binding proteins in these neurons may help to clarify the role of ambient  $\text{Ca}^{2+}$  binding proteins in CDI. Determination of the basal degree of CDI however will be complicated by the fact that several pathways converge on this mechanism (see below).

### The role of calmodulin

There is a longstanding notion that the limiting action of CDI on  $\text{Ca}^{2+}$  entry through HVA channels depends on calmodulin. Originally, a mechanism involving  $\text{Ca}^{2+}$ /calmodulin-dependent activation of calcineurin and subsequent dephosphorylation of HVA  $\text{Ca}^{2+}$  channel proteins was proposed [2]. More recent work has elaborated the role of calmodulin as a  $\text{Ca}^{2+}$  sensor that is bound constitutively to the channel protein and regulates CDI and even VDI by inducing complex conformational changes and utilizing the I-II linker as a common blocking particle [20, 33]. In accordance with these findings, blockers of calcineurin exerted a pronounced inhibitory effect on the degree of CDI in relay neurons. It has been shown previously that blockers of calcineurin also reduce CDI in relay neurons, thereby suggesting a role of channel dephosphorylation in this process [43]. The experimental conditions used in the present study do not allow

discrimination between the two possible modes of calmodulin action (i.e. direct action on the channel protein or activation of calcineurin). The finding that blockade of calmodulin exerts stronger effects on CDI than blockade of calcineurin [43] may indicate that calmodulin acts through both mechanisms in dLGN relay neurons.

### Involvement of the cytoskeleton

The cytoskeleton is a filamentous network of F-actin, microtubules and intermediate filaments and regulation of transmembrane ion flux is one of its important roles in cell signalling [28]. Results obtained from experiments in molluscan neurons [29] and hippocampal pyramidal neurons [30] have suggested that the cytoskeleton is involved in CDI. Although the transduction mechanism coupling the cytoskeleton to CDI is not fully understood and seems to differ between different cell types,  $\text{Ca}^{2+}$ -dependent destabilization of cytoskeletal elements that have a structural relationship to the channel protein has been suggested [4]. Cytoskeletal stabilizers reduced CDI in relay neurons. The microtubule stabilizer taxol was more effective than the microfilament stabilizer phalloidin, indicating that both cytoskeletal components are not involved equally in CDI. These data are in agreement with a model in which microtubules stabilize a microfilament lattice, with the latter probably binding directly to the  $\text{Ca}^{2+}$  channel complex [29, 30]. In this model the  $\text{Ca}^{2+}$  sensitivity of  $\text{Ca}^{2+}$  channels could be mediated by cytoskeletal depolymerization, since both microtubule and microfilament components of the cytoskeleton are disrupted by increases in the  $[\text{Ca}^{2+}]_i$ . It is interesting to note that a similar mechanism has been suggested for the  $\text{Ca}^{2+}$ -dependent reduction of NMDA receptor activity [56]. More experiments will have to clarify the uncoupling of CDI from  $\text{Ca}^{2+}$  entry during presence of cytoskeletal stabilizers and corroborate the above model in relay neurons.

### Involvement of HVA $\text{Ca}^{2+}$ channel subtypes

It is now recognized that CDI of L-type  $\text{Ca}^{2+}$  channels ( $\text{Ca}_v1.2$ ) is based on the activation of preassociated calmodulin in response to  $\text{Ca}^{2+}$  entry and is insensitive to the application of 10 mM BAPTA and thus suitable for the detection of local  $\text{Ca}^{2+}$  entry [39, 53, 55, 65]. In contrast, P/Q-type channels ( $\text{Ca}_v2.1$ ) possess a mechanistically related process of inactivation that is highly sensitive to the application of 0.5 mM EGTA and thus suitable for the detection of global  $\text{Ca}^{2+}$  entry [36, 39]. Other members of the  $\text{Ca}_v2$  family have been characterized as lacking or inconsistently showing CDI (N-type channels;  $\text{Ca}_v2.2$ ) whilst R-type channels ( $\text{Ca}_v2.3$ ) are basically devoid of CDI [60]. In agreement with this classical view L- and

P/Q-type  $\text{Ca}^{2+}$  channels but not N- and R-type channels have been found to be governed by CDI in relay neurons [42, 43]. Furthermore the inactivation of L-type, but not N-type, channels is influenced by phosphorylation/dephosphorylation [43] and  $\text{Ca}^{2+}$ -binding proteins (present study). In contrast to this classical view it has been recently demonstrated that N- and R-type channels possess a CDI mechanism very similar to that in P/Q-type channels [39]. In relay neurons CDI of P/Q-type channels is not sensitive to 1.1 mM EGTA while CDI of L-type channels is substantially blocked by 11 mM BAPTA [42]. Phenomena like clustering of  $\text{Ca}^{2+}$  channels which can lead to overlapping  $\text{Ca}^{2+}$  microdomains may obscure the strict segregation of local and global  $\text{Ca}^{2+}$  signalling and explain this discrepancy [6, 58].

#### Integrated view of CDI mechanisms and possible functional relevance

Different mechanisms underlying CDI have been described independently in different cell types [11]. Combining all experimental data of CDI in identified relay neurons [42, 43] (present study), it can be concluded for the first time that this feedback mechanism does not depend solely on a single process. Indeed, there is evidence for the involvement of calmodulin, several protein phosphatases and kinases, intracellular  $\text{Ca}^{2+}$ -binding proteins and the cytoskeleton, thereby indicating that a specific cell type can combine various mechanisms, highlighting the importance of this negative feedback signalling and pointing to an integrated model of CDI that has recently been suggested [11, 50].

HVA  $\text{Ca}^{2+}$  channels and thus CDI are relevant features during the tonic mode of activity and high-threshold oscillations in relay neurons [50].  $\text{Ca}^{2+}$  entry during tonic firing thus serves to activate further release of  $\text{Ca}^{2+}$  from intracellular stores [10], CDI [43] and  $\text{Ca}^{2+}$ -dependent  $\text{K}^{+}$  channels [7], thereby sustaining and shaping the processing of sensory information from the periphery to cortical structures. Furthermore, restriction of  $\text{Ca}^{2+}$  entry by CDI may be neuroprotective [13] and even life-sustaining [1]. The multitude of converging mechanisms in relay neurons offers multiple opportunities for modulating CDI, including the inhibition of CDI by the cAMP/PKA system [43]. This system is activated readily in relay neurons by transmitters (noradrenaline, serotonin) of the ascending brainstem system during wakefulness [41], thereby potentially strengthening the interplay between  $\text{Ca}^{2+}$  entry via HVA channels and intracellular  $\text{Ca}^{2+}$  stores that supports the relay mode. Future studies will have to unravel the different modulatory pathways that act upstream from the multiple CDI mechanisms thereby pointing to additional functions of CDI and unravelling further the elusive role of HVA  $\text{Ca}^{2+}$  channels in thalamic physiology.

**Acknowledgements** Supported by DFG (BU 1019/5-2; Leibniz-program to H.-C. P.). S. G. M. was a member of the DFG-Graduiertenkolleg "Biological basis of central nervous system diseases". Thanks are due to S. Mücke, A. Reusch, R. Ziegler, A. Ritter and A. Jahn for excellent technical assistance. The authors would like to thank F. Sieg for the help with the Western blot procedures.

#### References

1. Alseikhan BA, DeMaria CD, Colecraft HM, Yue DT (2002) Engineered calmodulins reveal the unexpected eminence of  $\text{Ca}^{2+}$  channel inactivation in controlling heart excitation. *Proc Natl Acad Sci USA* 99:17185–17190
2. Armstrong DL (1989) Calcium channel regulation by calneurin, a  $\text{Ca}^{2+}$ -activated phosphatase in mammalian brain. *Trends Neurosci* 12:117–122
3. Arnold DB, Heintz N (1997) A calcium responsive element that regulates expression of two calcium binding proteins in Purkinje cells. *Proc Natl Acad Sci USA* 94:8842–8847
4. Beck H, Steffens R, Heinemann U, Elger CE (1999)  $\text{Ca}^{2+}$ -dependent inactivation of high-threshold  $\text{Ca}^{2+}$  currents in hippocampal granule cells of patients with chronic temporal lobe epilepsy. *J Neurophysiol* 82:946–954
5. Berchtold MW, Brinkmeier H, Muntener M (2000) Calcium ion in skeletal muscle: its crucial role for muscle function, plasticity, and disease. *Physiol Rev* 80:1215–1265
6. Bertram R, Smith GD, Sherman A (1999) Modeling study of the effects of overlapping  $\text{Ca}^{2+}$  microdomains on neurotransmitter release. *Biophys J* 76:735–750
7. Biella G, Meis S, Pape H-C (2001) Modulation of a  $\text{Ca}^{2+}$ -dependent  $\text{K}^{+}$ -current by intracellular cAMP in rat thalamocortical relay neurons. *Thalamus & Related Systems* 1:157–167
8. Bradford MM (1976) A rapid and sensitive method for the quantitation of microgram quantities of protein utilizing the principle of protein-dye binding. *Anal Biochem* 72:248–254
9. Budde T, Mager R, Pape H-C (1992) Different types of potassium outward current in relay neurons acutely isolated from the rat lateral geniculate nucleus. *Eur J Neurosci* 4:708–722
10. Budde T, Sieg F, Braunewell KH, Gundelfinger ED, Pape H-C (2000)  $\text{Ca}^{2+}$ -induced  $\text{Ca}^{2+}$  release supports the relay mode of activity in thalamocortical cells. *Neuron* 26:483–492
11. Budde T, Meuth S, Pape H-C (2002) Calcium-dependent inactivation of neuronal calcium channels. *Nat Rev Neurosci* 3:873–883
12. Chard PS, Bleakman D, Christakos S, Fullmer CS, Miller RJ (1993) Calcium buffering properties of calbindin D28 k and parvalbumin in rat sensory neurones. *J Physiol (Lond)* 472:341–357
13. Choi DW (1994) Calcium and excitotoxic neuronal injury. *Ann NY Acad Sci* 747:162–171
14. Cimino M, Weiss B (1988) Characteristics of the binding of phenoxybenzamine to calmodulin. *Biochem Pharmacol* 37:2739–2745
15. Deschenes M, Paradis M, Roy JP, Steriade M (1984) Electrophysiology of neurons of lateral thalamic nuclei in cat: resting membrane properties and burst discharges. *J Neurophysiol* 51:1196–1219
16. Dixon WJ, Massey FJ (1969) Introduction to statistical analysis. McGraw Hill, New York
17. Dreessen J, Lutum C, Schafer BW, Heizmann CW, Knöpfel T (1996)  $\alpha$ -Parvalbumin reduces depolarization-induced elevations of cytosolic free calcium in human neuroblastoma cells. *Cell Calcium* 19:527–533
18. Eberhard M, Erne P (1994) Calcium and magnesium binding to rat parvalbumin. *Eur J Biochem* 222:21–26
19. Eckert R, Tillotson DL (1981) Calcium-mediated inactivation of the calcium conductance in caesium-loaded giant neurones of *Aplysia californica*. *J Physiol (Lond)* 314:265–280

20. Erickson MG, Liang H, Mori MX, Yue DT (2003) FRET two-hybrid mapping reveals function and location of L-type  $\text{Ca}^{2+}$  channel CaM preassociation. *Neuron* 39:97–107
21. Gabbott PL, Somogyi J, Stewart MG, Hamori J (1986) A quantitative investigation of the neuronal composition of the rat dorsal lateral geniculate nucleus using GABA-immunocytochemistry. *Neuroscience* 19:101–111
22. Gander JC, Gotzos V, Fellay B, Schwaller B (1996) Inhibition of the proliferative cycle and apoptotic events in WiDr cells after down-regulation of the calcium-binding protein calretinin using antisense oligodeoxynucleotides. *Exp Cell Res* 225:399–410
23. Gera S, Byerly L (1999) Voltage- and calcium-dependent inactivation of calcium channels in *Lymnaea* neurons. *J Gen Physiol* 114:535–550
24. Grossman A, Lieberman AR, Webster KE (1973) A Golgi study of the rat dorsal lateral geniculate nucleus. *J Comp Neurol* 150:441–466
25. Heine M, Ponimaskin E, Bickmeyer U, Richter DW (2002) 5-HT-receptor-induced changes of the intracellular cAMP level monitored by a hyperpolarization-activated cation channel. *Pflügers Arch* 443:418–426
26. Hering S, Berjukow S, Sokolov S, Marksteiner R, Weiss RG, Kraus R, Timin EN (2000) Molecular determinants of inactivation in voltage-gated  $\text{Ca}^{2+}$  channels. *J Physiol (Lond)* 528:237–249
27. Hubbard MJ, McHugh NJ (1995) Calbindin28 kDa and calbindin30 kDa (calretinin) are substantially localised in the particulate fraction of rat brain. *FEBS Lett* 374:333–337
28. Janmey PA (1998) The cytoskeleton and cell signaling: component localization and mechanical coupling. *Physiol Rev* 78:763–781
29. Johnson BD, Byerly L (1993) A cytoskeletal mechanism for  $\text{Ca}^{2+}$  channel metabolic dependence and inactivation by intracellular  $\text{Ca}^{2+}$ . *Neuron* 10:797–804
30. Johnson BD, Byerly L (1994)  $\text{Ca}^{2+}$  channel  $\text{Ca}^{2+}$ -dependent inactivation in a mammalian central neuron involves the cytoskeleton. *Pflügers Arch* 429:14–21
31. Jones SW (2003) Calcium channels: unanswered questions. *J Bioenerg Biomembr* 35:461–475
32. Kay AR (1991) Inactivation kinetics of calcium currents of acutely dissociated CA1 pyramidal cells of the mature guinea-pig hippocampus. *J Physiol (Lond)* 437:27–48
33. Kim J, Ghosh S, Nunziato DA, Pitt GS (2004) Identification of the components controlling inactivation of voltage-gated  $\text{Ca}^{2+}$  channels. *Neuron* 41:745–754
34. Lader AS, Kwiatkowski DJ, Cantiello HF (1999) Role of gelsolin in the actin filament regulation of cardiac L-type calcium channels. *Am J Physiol* 277:C1277–C1283
35. Lee A, Wong ST, Gallagher D, Li B, Storm DR, Scheuer T, Catterall WA (1999)  $\text{Ca}^{2+}$ /calmodulin binds to and modulates P/Q-type calcium channels. *Nature* 399:155–159
36. Lee A, Scheuer T, Catterall WA (2000)  $\text{Ca}^{2+}$ /calmodulin-dependent facilitation and inactivation of P/Q-type  $\text{Ca}^{2+}$  channels. *J Neurosci* 20:6830–6838
37. Lee A, Westenbroek RE, Haeseleer F, Palczewski K, Scheuer T, Catterall WA (2002) Differential modulation of  $\text{Ca}_v2.1$  channels by calmodulin and  $\text{Ca}^{2+}$ -binding protein 1. *Nat Neurosci* 5:210–217
38. Levitan IB (1999) It is calmodulin after all! Mediator of the calcium modulation of multiple ion channels. *Neuron* 22:645–648
39. Liang H, DeMaria CD, Erickson MG, Mori MX, Alseikhan BA, Yue DT (2003) Unified mechanisms of  $\text{Ca}^{2+}$  regulation across the  $\text{Ca}^{2+}$  channel family. *Neuron* 39:951–960
40. Magloczky Z, Freund TF (1995) Delayed cell death in the contralateral hippocampus following kainate injection into the CA3 subfield. *Neuroscience* 66:847–860
41. McCormick DA (1992) Neurotransmitter actions in the thalamus and cerebral cortex and their role in neuromodulation of thalamocortical activity. *Prog Neurobiol* 39:337–388
42. Meuth SG, Budde T, Pape H-C (2001) Differential control of high-voltage activated  $\text{Ca}^{2+}$  current components by a  $\text{Ca}^{2+}$ -dependent inactivation mechanism in thalamic relay neurons. *Thalamus & Related Systems* 1:31–38
43. Meuth SG, Pape H-C, Budde T (2002) Modulation of  $\text{Ca}^{2+}$  currents in rat thalamocortical relay neurons by activity and phosphorylation. *Eur J Neurosci* 15:1603–1614
44. Meyers MB, Puri TS, Chien AJ, Gao T, Hsu PH, Hosey MM, Fishman GI (1998) Sorcin associates with the pore-forming subunit of voltage-dependent L-type  $\text{Ca}^{2+}$  channels. *J Biol Chem* 273:18930–18935
45. Munsch T, Budde T, Pape H-C (1997) Voltage-activated intracellular calcium transients in thalamic relay neurons and interneurons. *Neuroreport* 8:2411–2418
46. Nägerl UV, Mody I, Jeub M, Lie AA, Elger CE, Beck H (2000) Surviving granule cells of the sclerotic human hippocampus have reduced  $\text{Ca}^{2+}$  influx because of a loss of calbindin-D<sub>28k</sub> in temporal lobe epilepsy. *J Neurosci* 20:1831–1836
47. Naraghi M, Neher E (1997) Linearized buffered  $\text{Ca}^{2+}$  diffusion in microdomains and its implications for calculation of  $[\text{Ca}^{2+}]$  at the mouth of a calcium channel. *J Neurosci* 17:6961–6973
48. Ohara PT, Lieberman AR, Hunt SP, Wu JY (1983) Neural elements containing glutamic acid decarboxylase (GAD) in the dorsal lateral geniculate nucleus of the rat; immunohistochemical studies by light and electron microscopy. *Neuroscience* 8:189–211
49. Pape H-C, Budde T, Mager R, Kisvarday Z (1994) Prevention of  $\text{Ca}^{2+}$ -mediated action potentials in GABAergic local circuit neurons of the thalamus by a transient  $\text{K}^{+}$  current. *J Physiol (Lond)* 478:403–422
50. Pape H-C, Munsch T, Budde T (2004) Novel vistas of calcium-mediated signalling in the thalamus. *Pflügers Arch* 448:131–138
51. Patz S, Grabert J, Gorba T, Wirth MJ, Wahle P (2004) Parvalbumin expression in visual cortical interneurons depends on neuronal activity and TrkB ligands during an early period of postnatal development. *Cereb Cortex* 14:342–351
52. Payne ME, Fong YL, Ono T, Colbran RJ, Kemp BE, Soderling TR, Means AR (1988) Calcium/calmodulin-dependent protein kinase II. Characterization of distinct calmodulin binding and inhibitory domains. *J Biol Chem* 263:7190–7195
53. Peterson BZ, DeMaria CD, Adelman JP, Yue DT (1999) Calmodulin is the  $\text{Ca}^{2+}$  sensor for  $\text{Ca}^{2+}$ -dependent inactivation of L-type calcium channels. *Neuron* 22:549–558
54. Pusch M, Neher E (1988) Rates of diffusional exchange between small cells and a measuring patch pipette. *Pflügers Arch* 411:204–211
55. Qin N, Olcese R, Bransby M, Lin T, Birnbaumer L (1999)  $\text{Ca}^{2+}$ -induced inhibition of the cardiac  $\text{Ca}^{2+}$  channel depends on calmodulin. *Proc Natl Acad Sci USA* 96:2435–2438
56. Rosenmund C, Clements JD, Westbrook GL (1993) Nonuniform probability of glutamate release at a hippocampal synapse. *Science* 262:754–757
57. Rousset M, Cens T, Gavarini S, Jeromin A, Charnet P (2003) Down-regulation of voltage-gated  $\text{Ca}^{2+}$  channels by neuronal calcium sensor-1 is beta subunit-specific. *J Biol Chem* 278:7019–7026
58. Sherman A, Keizer J, Rinzel J (1990) Domain model for  $\text{Ca}^{2+}$ -inactivation of  $\text{Ca}^{2+}$  channels at low channel density. *Biophys J* 58:985–995
59. Smith MK, Colbran RJ, Soderling TR (1990) Specificities of autoinhibitory domain peptides for four protein kinases. Implications for intact cell studies of protein kinase function. *J Biol Chem* 265:1837–1840
60. Soldatov NM (2003)  $\text{Ca}^{2+}$  channel moving tail: link between  $\text{Ca}^{2+}$ -induced inactivation and  $\text{Ca}^{2+}$  signal transduction. *Trends Pharmacol Sci* 24:167–171
61. Steriade M, Deschenes M (1984) The thalamus as a neuronal oscillator. *Brain Res Rev* 8:1–63
62. Stotz SC, Zamponi GW (2001) Structural determinants of fast inactivation of high voltage-activated  $\text{Ca}^{2+}$  channels. *Trends Neurosci* 24:176–181

63. Van den Bosch L, Van Damme P, Vleminckx V, Van Houtte E, Lemmens G, Missiaen L, Callewaert G, Robberecht W (2002) An  $\alpha$ -mercaptoacrylic acid derivative (PD150606) inhibits selective motor neuron death via inhibition of kainate-induced  $\text{Ca}^{2+}$  influx and not via calpain inhibition. *Neuropharmacology* 42:706–713
64. Zhou Q, Godwin DW, O'Malley DM, Adams PR (1997) Visualization of calcium influx through channels that shape the burst and tonic firing modes of thalamic relay neurons. *J Neurophysiol* 77:2816–2825
65. Zühlke RD, Pitt GS, Deisseroth K, Tsien RW, Reuter H (1999) Calmodulin supports both inactivation and facilitation of L-type calcium channels. *Nature* 399:159–162